PROBABILITY FUNCTIONAL EVALUATION OF CHEST INJURY BASED ON RIB STRAIN OF HUMAN BODY MODEL IN FRONTAL COLLISION

Yoshiki Takahira
Shizue Katsumata
Takeshi Yamamoto
Mitsutoshi Masuda
Toyota Motor Corporation
Japan

Paper Number 23-0218

ABSTRACT

This study examined the influence of chest restraint force on the chest injury probability of the human body model (HBM) in frontal collision. Total Human Model for Safety (THUMS) Version 4.1 AM50 was seated in the driver's seat of a finite element (FE) model represented a prototype midsize vehicle, and frontal collision simulations were performed. The probability of three or more rib fractures from 20YO to 80YO were predicted from simulated THUMS rib strain based on prior work. The probability increased with age, and showed a tendency to rise sharply beginning around the 60YO in particular. The trend was shown to be similar to the probability predicted statistically from the NASS-CDS field accident data. Furthermore, a collision simulation was also conducted in which the restraint balance between the seatbelt and airbag was changed while keeping the same amount of forward excursion of the occupant. As a result, it was found that the probability of rib fracture was reduced by the combination of reducing the seatbelt force and increasing the initial restraint force of the airbag compared to a base specification. This was due to the improved ride-down efficiency and reduced seatbelt contact force, which reduced the strain on the upper ribs on the path of seatbelt.

INTRODUCTION

Frontal collisions account for a high proportion of fatal crashes involving vehicle occupants. Chest injury is the most common cause of death and injury among belted occupants. It has been reported that the ribs deflect due to strong external force on the chest, causing pulmonary contusion and aortic injury [1]. In addition, if multiple ribs are fractured, normal chest wall function becomes difficult, which is called flail chest, and respiratory failure may occur. In recent years, CAE simulation using HBMs has been utilized to investigate the mechanism of chest injury and research safety technology. HBMs are modeled the geometry and characteristics of the human chest with reference to the anatomy. They have the advantage of being able to simulate the boney and organ strain. Kitagawa et al. evaluated the effects of four-point shoulder belts and air belts with THUMS Version 4 and Mroz et al. evaluated the effects of 3 + 2 criss-cross belts and split buckles with the Elderly THUMS TUC, using rib bone strain. However, most of HBMs refer to the shape data of a specific individual, and there is a large dependence on the model shape so even with the same body size. In addition, the stress-strain characteristics and bone thickness of ribs are greatly affected by individual differences and age differences [5-6], further complicating issues in quantitative injury evaluation with HBMs. Therefore, Forman et al. developed a methodology for predicting the probability of an arbitrary number of rib fractures from the rib strain of HBM using a probability function adjusted based on the results of thoracic impactors, seatbelt compressions, sled tests, etc. using Post Modern Human Subject (PMHS) [7-8]. It is expected that equivalent evaluation of chest injury probability will be possible even if different HBMs such as THUMS, The Global Human Body Models Consortium (GHBMC), and SAFER HBM are used.
In this study, CAE simulations were performed using the THUMS Version 4.1 AM50 occupant model to assume a frontal collision of a medium-sized vehicle, and the probability of three or more rib fractures was predicted based on the rib strain obtained by simulation. To validate the probability, results were compared

with the probability of 3 or more rib fractures in a medium-sized male in frontal collision calculated by Forman et al. using the NASS-CDS field accident database [8]. Furthermore, using this simulation model, the probability of chest injury was predicted for three different restraint balance patterns of seatbelts and airbags, and the factors that caused the difference in the injury probability due to the applied force to the chest were investigated.

METHOD

Frontal Collision Simulation

The simulations were performed using FE models. The LS-DYNATM Version 971 was used for the FE analysis solver developed by Ansys (US). The vehicle frontal collision simulations were performed using the THUMS Version 4.1 AM50 occupant model (Figure 1). The occupant model represents a medium-sized male occupant with a height of 178 cm and a weight of 75 kg, about 35 years old. The model describes the anatomical features of human body, including the major skeletal structure, articular ligaments, brain, internal organs and other soft tissues. THUMS' mechanical responses were validated for various loading cases using PMHS test data described in the literatures [9-11]. A FE model representing the driver's seat of a medium-sized car was used, and an acceleration pulse for a frontal collision was applied. The interior parts (steering, instrument panel, pedals, seats, seatbelt and airbags) that could come into contact with the occupants were assumed to be deformable, while the windshield and floor panel were assumed to be rigid. The seatbelt retractor model simulated the functions of a pre-tensioner and a load-limiter. The deployment of the driver airbag (DAB) and knee airbag (KAB) was also simulated. The occupant behavior in the simulation model is consistent with the result of sled test using PMHS conducted by Albert et al. [12-14].

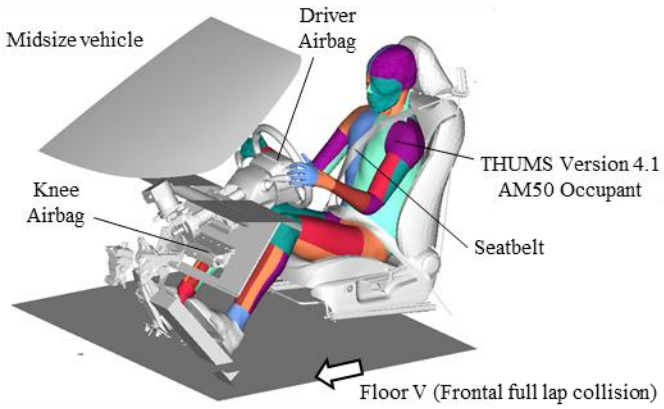

Figure 1. THUMS frontal collision simulation model

Simulation Matrix

A total of six simulations were conducted: two cases of speed change (delta V) of 40 km/h and 56 km/h; three cases of restraint system specifications with different restraint balances between seatbelt and DAB (Figure 2, 3, Table 1). A general seatbelt load limiter and DAB were utilized in Base. Spec. A reduced the load limiter by 25% compared to Base. Spec. B increased the deployment depth by 25% without increasing the volume of the DAB compared to Spec. A. The internal pressure was adjusted so that the amount of the chest forward excursion in a collision with delta V of 56 km/h was equivalent to Base. The specifications of these three types of restraint systems are for research only and do not represent the characteristics of actual products.

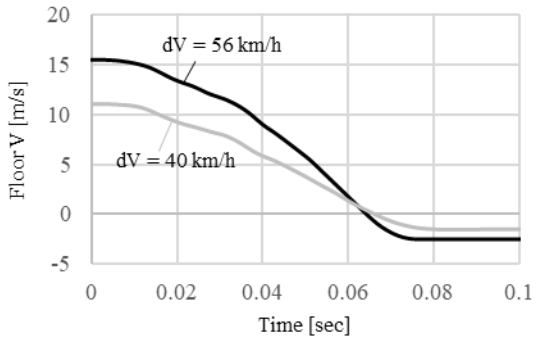

Figure 2. Time history of floor V in frontal full overlap collision

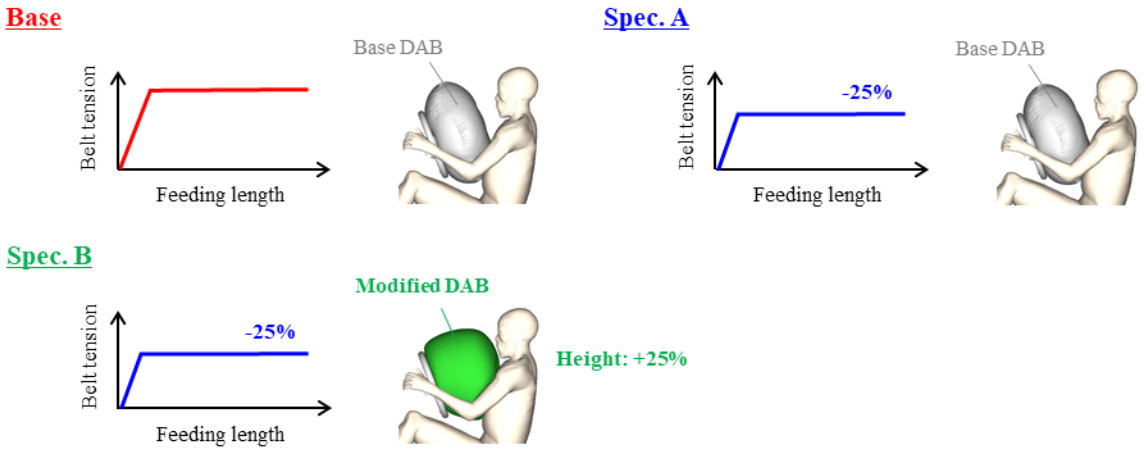

Figure 3. Specification of restraint system

Table 1.
Simulation matrix

Case	Delta V	Restraint system
#1	40 km/h	Base
#2	↑	Spec. A
#3	↑	Spec. B
#4	56 km/h	Base
#5	↑	Spec. A
#6	↑	Spec. B

Prediction of Chest Injury Probability by THUMS

The probability of three or more rib fractures (AIS3+) from the principal strain of the rib cortical bones obtained from the simulation was calculated using the chest injury probability function for THUMS proposed by Forman et al. (Figure 4). In this methodology, the fracture probability for each of the 12 left and right ribs is first obtained from the relationship between the principal strain 95tile (MPS95) of the ribs and the fracture probability adjusted based on the results of the PMHS tests. Next, the probability of any number of fractures is calculated using the generalized binomial model. An age term is included in this function, and with increasing age there is a higher probability of fracture at lower strains.

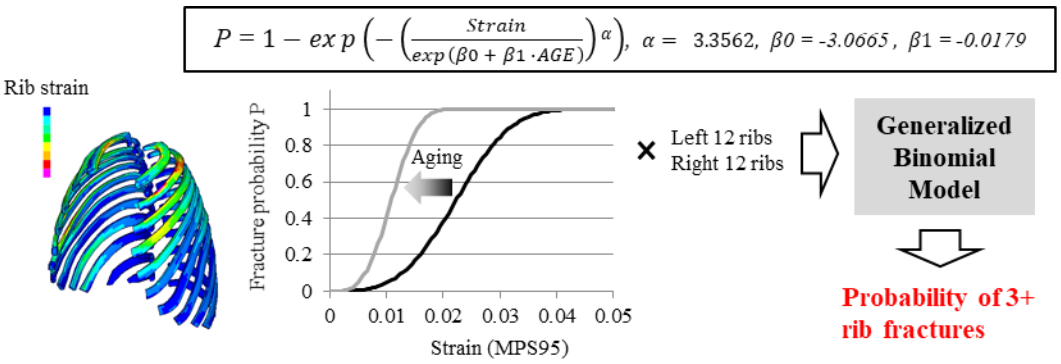

Figure 4. Chest injury probability function for THUMS V4.1 [8]

RESULTS

Occupant Kinematics

Figure 5 shows the occupant kinematics at maximum forward excursion of the chest. The numerical values in the figure represent the amount of chest (T4) excursion based on the floor. At delta V of 40 km/h, the chest excursion in base was 322 mm, while it increased to 351 mm with Spec. A, which has reduced belt tension compared to Base. Furthermore, that in Spec. B, which increased the deployment depth of the DAB compared to Spec. A, was 295 mm, which was 56 mm less than Spec. A. At delta V of 56 km/h, the amount of chest excursion in Base was 429 mm, while it increased to 466 mm with Spec. A. And that in Spec. B was 422 mm, 54 mm less than in Spec. A, which was the same as Base (as intended).

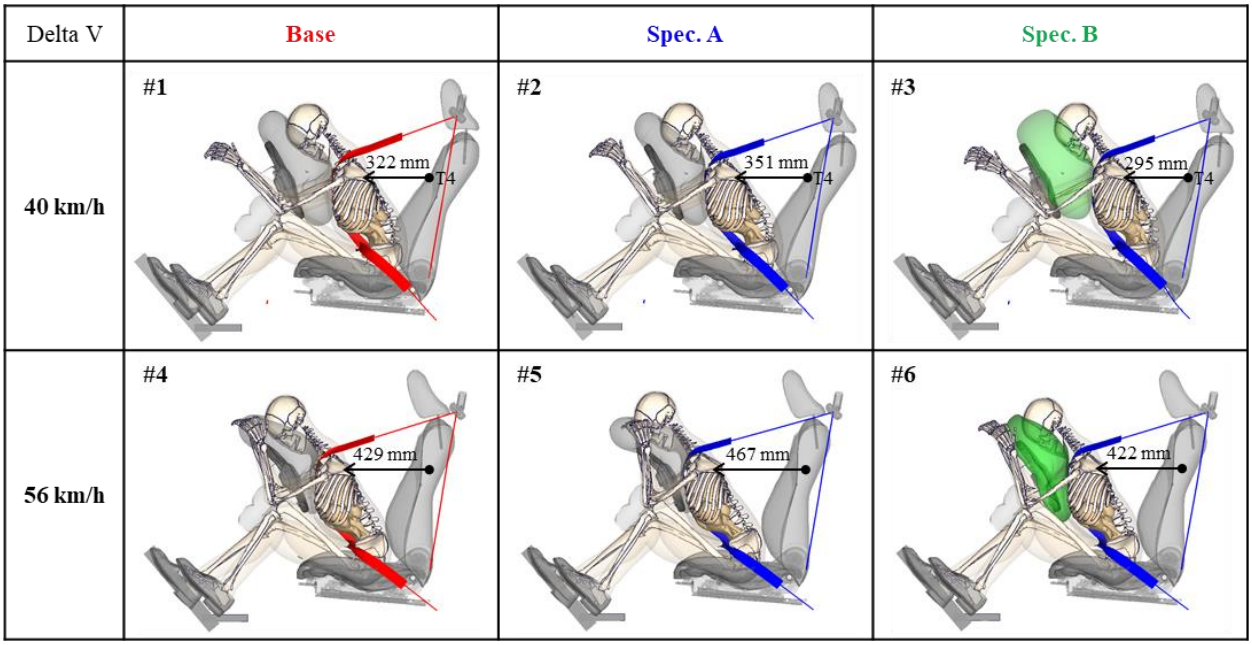

Figure 5. Occupant kinematics at maximum chest excursion

Applied Force to Anterior Chest

Figure 6 shows the force-stroke curve of the contact force applied to the anterior chest from the seatbelt and DAB and with respect to the amount of chest excursion. In Spec. A, which reduced the belt tension compared to Base, the belt contact force decreased from 5 kN to 4 kN, however the DAB contact force increased from

1.6 kN to 2 kN due to the increase in chest excursion. In addition, in Spec. B, which increased the DAB deployment depth compared to Spec. A, the amount of chest excursion decreased, but both the belt and DAB contact force were slightly reduced compared to Spec. A. At delta V of 56 km/h, Spec. A reduced the belt contact force from 6.4 kN to 5.2 kN compared to Base, however the DAB contact force increased from 3.5 kN to 4.2 kN. In Spec. B, the belt contact force decreased from 5.2 kN to 4.7 kN, and the DAB contact force decreased from 4.2 kN to 3.5 kN. compared to Spec. A.

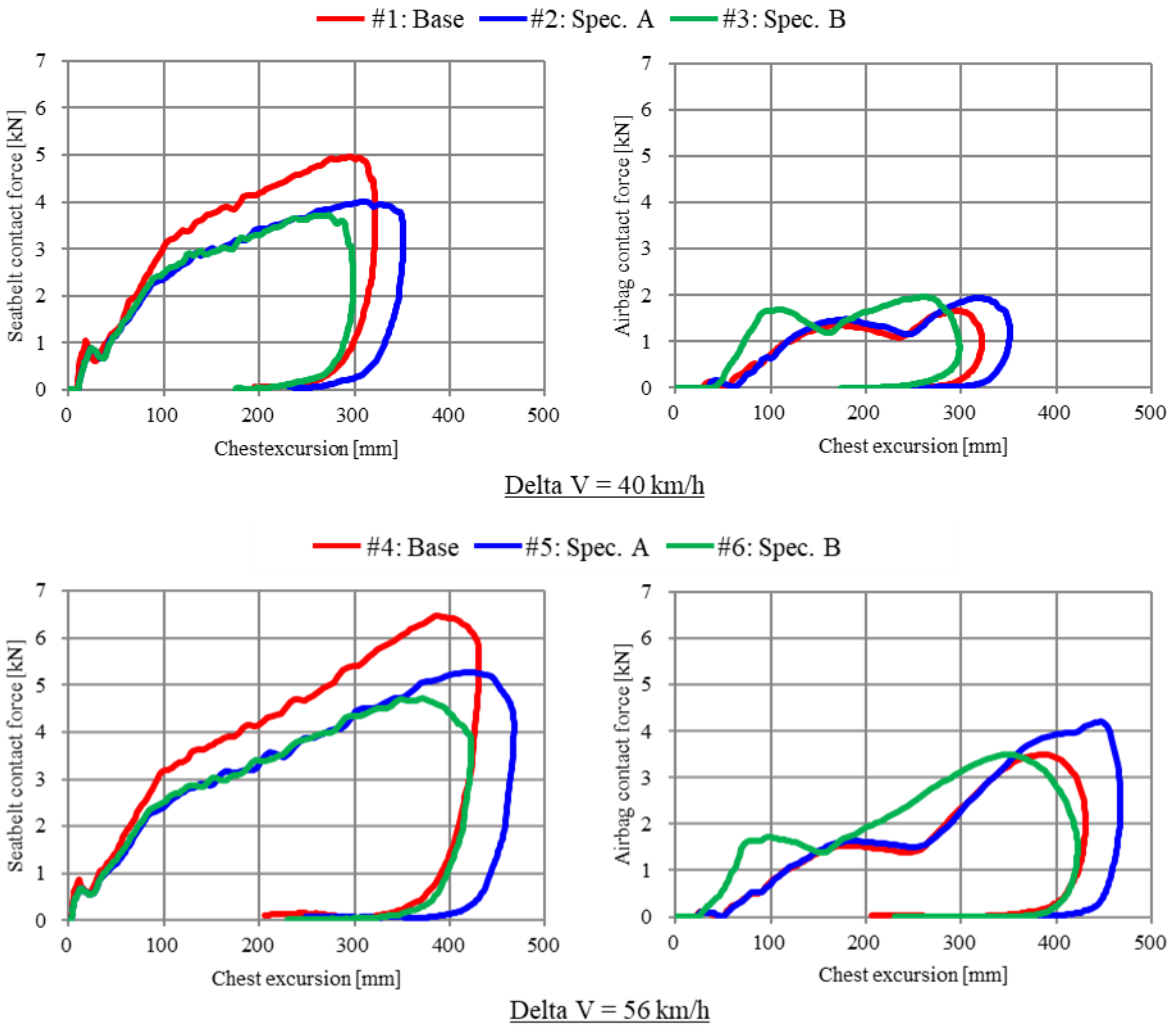

Figure 6. Chest applied force and excursion curve in CAE simulation

Rib Strain

Figure 7 shows the maximum principal strain distribution of the rib cortical bone, and Figure 8 shows the MPS95 of each ribs. In all cases, the left upper ribs, where the seatbelt was attached, tended to exhibit the most strain, and the strain level was generally higher at delta V = 56 km/h compared to delta V of 40 km/h. At delta V of 40 km/h, there was no difference in the strain level in all three cases. On the other hand, at delta V of 56 km/h, the strain level of Spec. A, which reduced the belt force, was the almost same as that of Base. However, in Spec. B, which had the higher deployment depth of the DAB, the amount of strain at left first rib was particularly reduced.

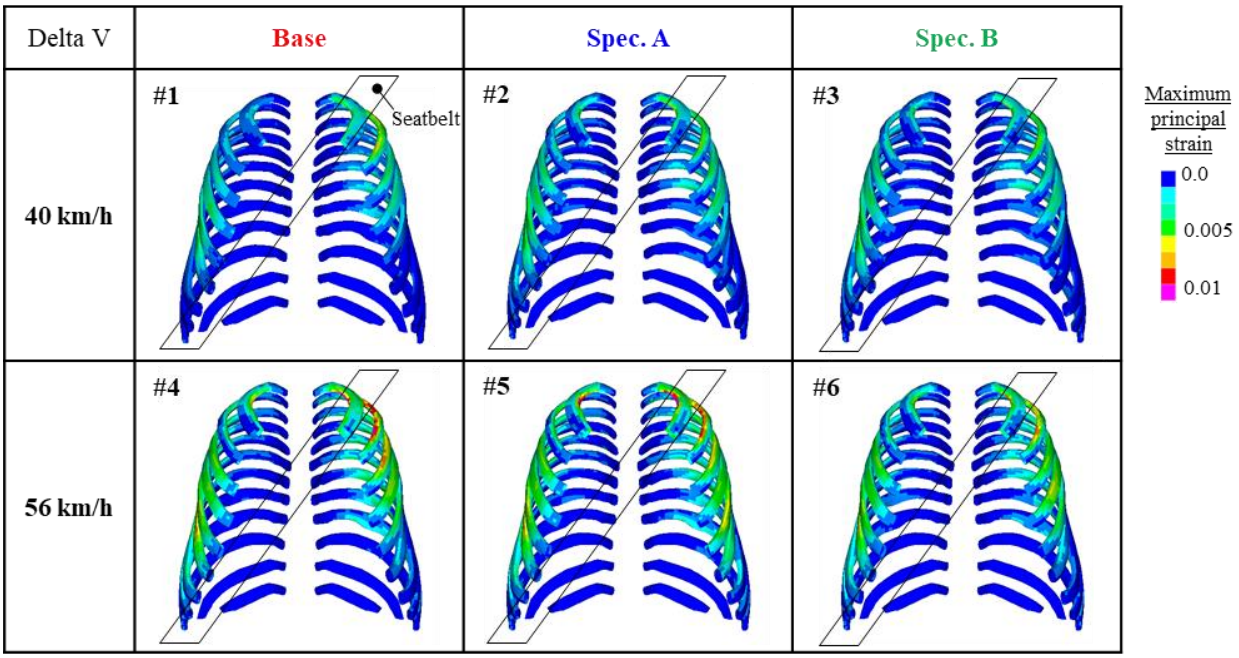

Figure 7. Maximum principal strain distribution rib cortical bones

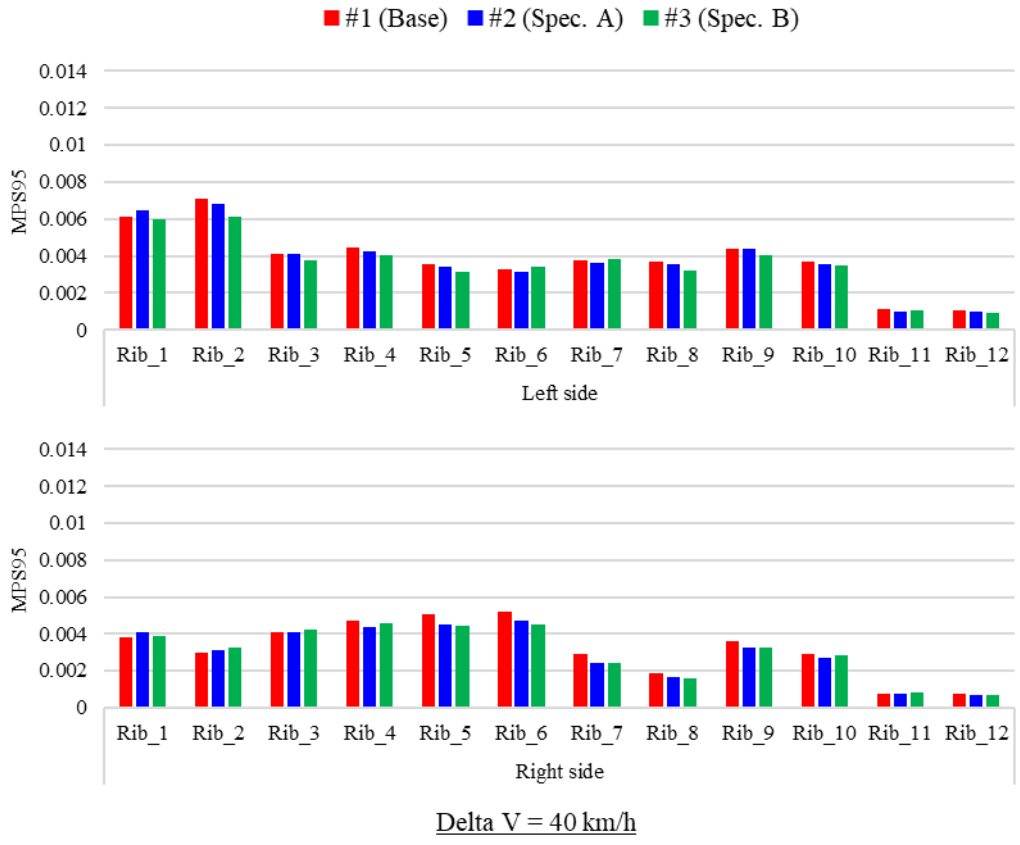

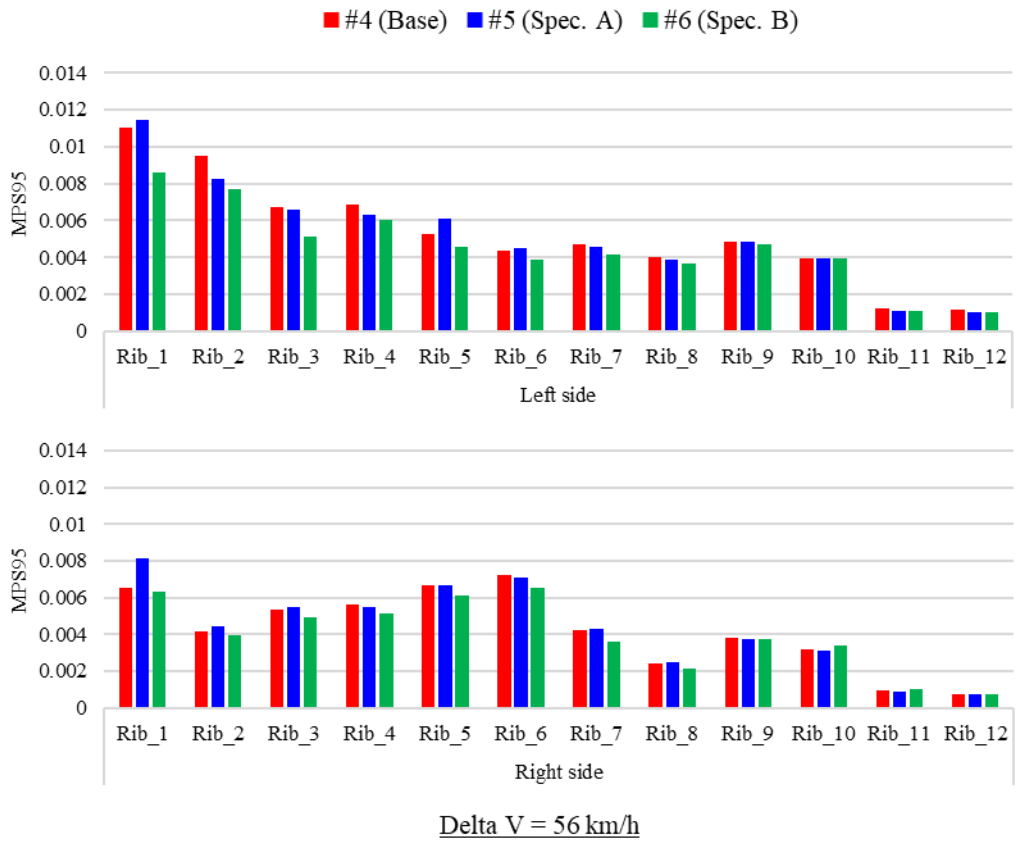

Figure 8. 95%tile of maximum principal strain(MPS95)

Chest Injury Probability

Figure 9 shows the probability of 3 or more rib fractures (AIS3+) calculated based on the rib strain obtained from the simulations. The horizontal axis represents the age of the occupant, and the vertical axis represents the probability. At delta V of 40km/h, the probability was almost 0 until 60YO and was below 5% even 80YO. On the other hand, at delta V of 56 km/h, the probability increased around 50YO, and it increased to nearly 20% at 70YO and to about 50% at 80YO in Base case. In addition, the probability of Spec. A with reduced belt force was almost same as Base regardless of age. Furthermore, the probability of Spec. B, which had the higher deployment depth of DAB, was reduced to about 5% at 70YO and about 25% at 80YO.

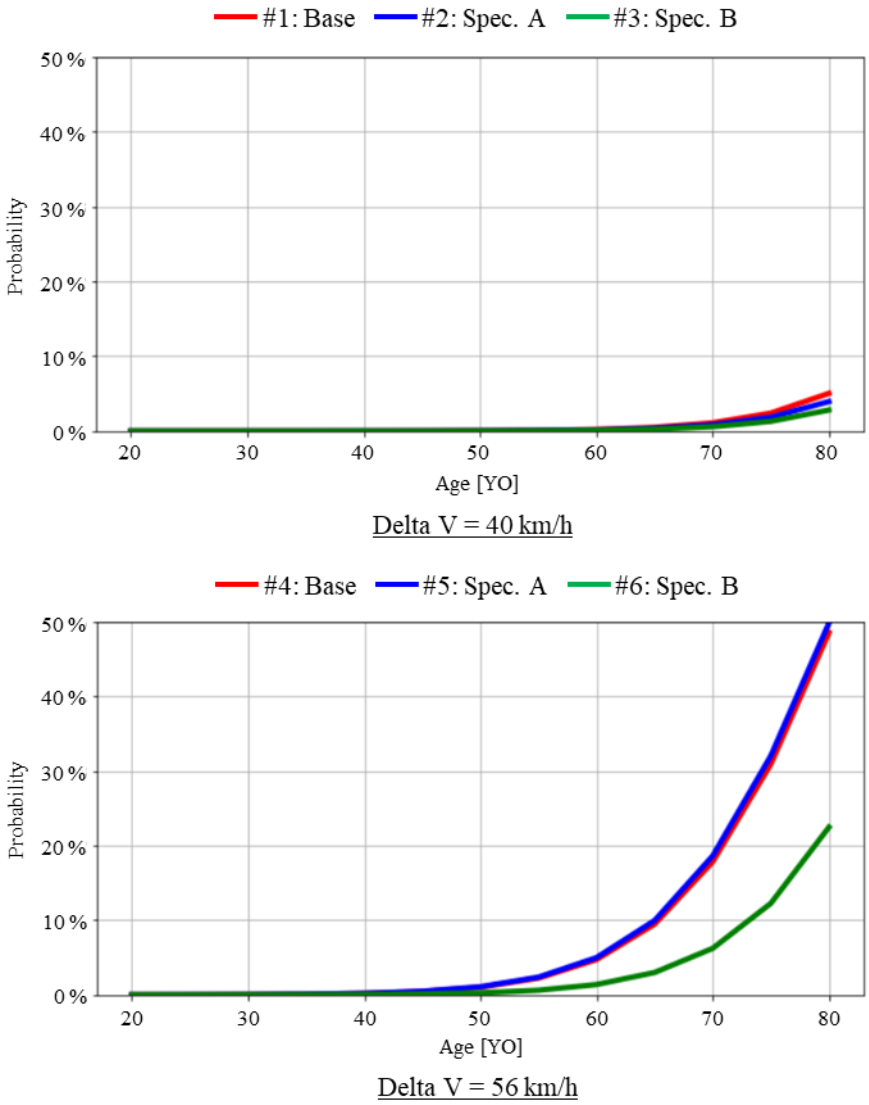

Figure 9. Probability of 3+ rib fractures

DISCUSSION

Validation of Chest Injury Probability of THUMS Simulation

Rib fracture probability calculated from the rib strain obtained in the frontal collision simulation using THUMS (#4) were compared with the probability statistically predicted from the NASS-CDS field crash database by Forman et al. [8] (Figure 10). Both results show the probability of 3 or more rib fractures for medium-sized male occupants aged 25, 45, and 65 in frontal collisions with delta V of 56 km/h. At the ages of 25 and 45, the simulation results were both less than 0.1%, and the results from crash data were 0.3% and 1.3%, respectively, both with probabilities close to zero. On the other hand, at 65YO, the simulation result increased to 9.5% and result from crash data increased to 6.2%, showing a similar trend.

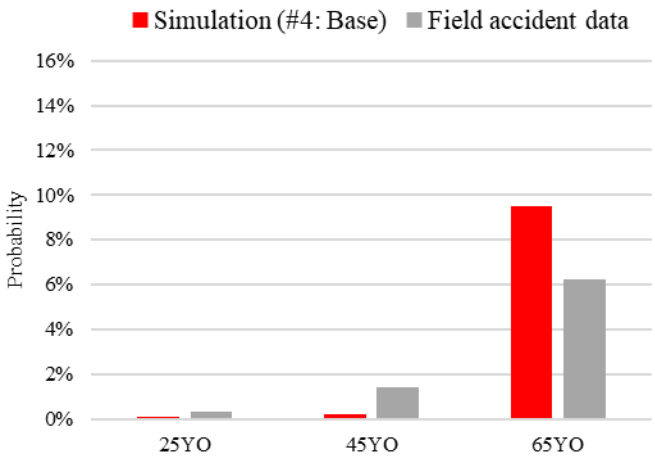

Figure 10. Probability of 3+ rib fractures in 56 km/h frontal collision

Influence of Restraint Balance on Chest Injury Probability

The probability of three or more rib fractures calculated from the rib strain distribution of THUMS was compared with three specifications with different restraint balances of the seatbelt and DAB. The left upper ribs, which exhibited the most strain, were deformed mainly by the clavicle intrusion due to the applied force from the seatbelt and airbag (Figure 11). At delta V of 56 km/h, no reduction in fracture probability was observed with Spec. A, which has a lower belt tension than Base. Although the applied force to the chest from the seatbelt decreased, the DAB reaction force increased due to the increase of chest excursion. As a result, the reduction of the total applied force to the chest was as small as 5% (Figure 12), with no reduction in the amount of clavicle deformation. In contract, in Spec. B, which combines a reduction in belt tension and an increase in DAB deployment depth, the fracture probability decrease by half. The increase in the initial restraint force of the DAB increased the ride-down efficiency and decreased the amount of chest excursion (Table 2). Therefore, both the seatbelt and DAB contact forces were reduced compared to Spec. A. As a result, the reduction rate of the total applied force to the chest compared to Base was as large as 18%, and the amount of clavicle deformation was reduced. It was indicated that a lower belt force is more effective in reducing the risk of rib fracture if the amount of chest excursion is similar.

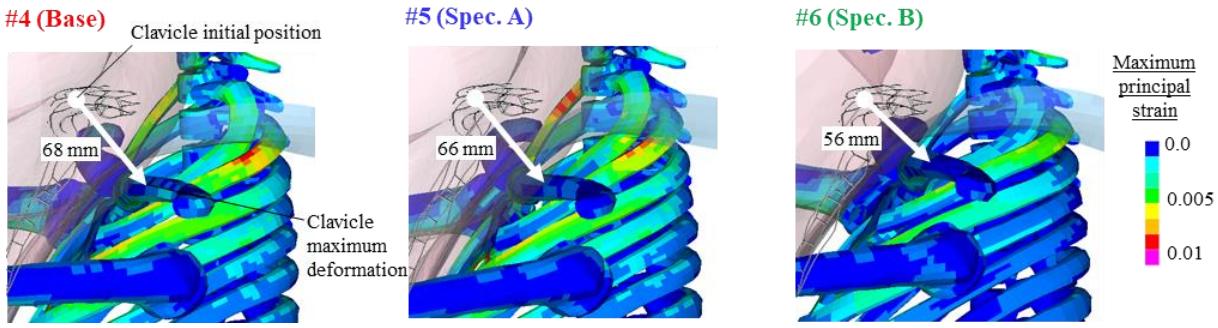

Figure 11. Deformed shape of scapula and upper ribs wrt. thoracic spine in 56 km/h frontal collision

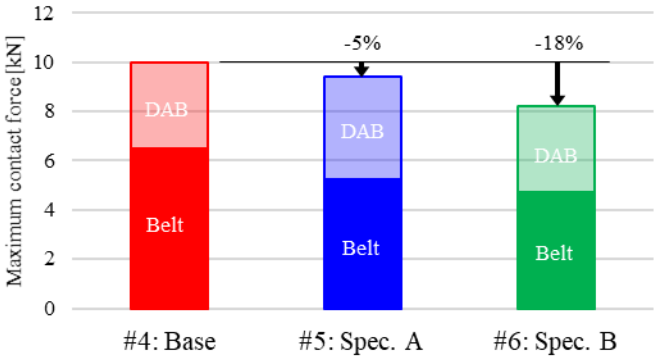

Figure 12. Maximum applied force to anterior chest in 56 km/h frontal collision

Table 2.
Ride-down efficiency of chest restraint in 56 km/h frontal collision

#4: Base	#5: Spec. A	#6: Spec. B
30.3%	25.4%	33.5%

LIMITATION

This study assumed a particular sitting posture and position for each occupant model, but of course this may vary among individuals and in specific situations. Interaction with restraint systems is also influenced by such factors. In addition, the prediction of rib fracture probability using field crash data includes various vehicle information, and of course it differs from the vehicle model used in this simulation, so further validations are necessary.

CONCLUSIONS

The rib fracture probability function proposed by Forman et al. was used to calculate the probability of three or more rib fractures, using the rib strain predicted by the frontal collision simulation using the THUMS Version 4.1 AM50 occupant model. Since the results showed a similar tendency to the prediction results of the field crash data, it was estimated that the prediction accuracy of the simulations were sufficient. Using this model, simulations with different restraint balances between seatbelt and DAB were performed. Compared to the base restraint system, the specification reducing only seatbelt force did not produce substantial reduction effect of the rib fracture probability. On the other hand, the specification that also included increasing the initial restraint force of the DAB to keep the same amount of chest forward excursion was effective in reducing the rib fracture probability. This study demonstrated the difference in rib fracture probability with different restraint systems, so this methodology is effective technology for future virtual assessment of crash safety.

REFERENCES

[1] Tominaga, S., Nishimoto, T., Motomura, T., Mashiko, K., Sakamoto, Y. 2012. “Analysis of Thoracoabdominal Injury based on Japan Trauma Data Bank and In-depth Accident Study.” Transactions of Society of Automotive Engineers of Japan, 43(2)

[2] Japanese Association for Acute Medicine. “Glossary of medical terms.” Internet: https://www.jaam.jp/dictionary/dictionary/word/0406.html

[3] Kitagawa, Y., Yasuki, T. 2013. “Correlation among Seatbelt Load, Chest Deflection, Rib Fracture and Internal Organ Strain in Frontal Collisions with Human Body Finite Element Models.” Proceedings of 2013 IRCOBI Conference

[4] Mroz, K., Pipkorn, B., Sunnevang, C., Eggers, A., & Brase, D. 2018. “Evaluation of Adaptive Belt Restraint Systems for the Protection of Elderly Occupants in Frontal Impacts.” Proceedings of 2018 IRCOBI Conference
[5] Courtney, C., Hayes, C., & Gibson, J. 1996. “Age-Related Differences in Post-Yield Damage in Human Cortical Bone. Experiment and Model.” Journal of Biomechanics, 29(11)
[6] McCalden, R. W., McGeough, J. A., Barker, M. B., & Court-Brown, C. M. 1993. “Age-Related Changes in The Tensile Properties of Cortical Bone. Journal of Bone and Joint Surgery.” 75-A
[7] Forman, J., Kent, Mroz, K., Pipkorn, B., Bostrom, O., Segui-Gomez, M. 2012. “Predicting Rib Fracture Risk with Whole-Body Finite Element Models: Development and Preliminary Evaluation of a Probabilistic Analytical Framework.” Proceedings of the 56th AAAM Annual Conference on Annuals of Advances in Automotive Medicine
[8] Forman, J., Kulkarni, S., Perez-Rapela, D., Mukherjee, S., Panzer, M., & Hallman, J. 2022. “A Method for Thoracic Injury Risk Function Development for Human Body Models.” Proceedings of 2022 IRCOBI Conference
[9] Watanabe, R., Miyazaki, H., Kitagawa, Y., & Yasuki, T. 2012. “Research of the relationship of pedestrian Injury to collision speed, car-type, impact location and pedestrian sizes using human FE model (THUMS Version 4).” Stapp Car Crash Journal, 561
[10] Shigeta, K., Kitagawa, Y., & Yasuki, T. 2009. “Development of next generation human FE model capable of organ injury prediction.” Proceedings of the 21st ESV Conference
[11] Kitagawa, Y., Hayashi, S., Yamada, K., & Gotoh, M. 2017. “Occupant kinematics in simulated autonomous driving vehicle collisions, direction and angle.” Stapp Car Crash Journal, 61
[12] Albert, D., Beeman, S., & Kemper, A. 2018. “Occupant kinematics of the Hybrid III, THOR-M, and postmortem human surrogates under various restraint conditions in full-scale frontal sled tests.” Traffic Injury Prevention, 19(S1)
[13] Albert, D., Beeman, S., & Kemper, A. 2018. “Assessment of Thoracic Response and Injury Risk Using the Hybrid III, THOR-M, and Post-Mortem Human Surrogates under Various Restraint Conditions in Full-Scale Frontal Sled Tests.” Stapp Car Crash Journal, 62
[14] Takahira, Y., Akima, S., Kusuhara, Y., Tanase, N., & Kitagawa, Y. 2021. “Cross-Sectional Analysis of Rib Fracture Mechanism of Elderly Occupant in Frontal Collision using THUMS.” Proceedings of 2021 IRCOBI Conference